Distribution system with wind penetration

Sistema de distribución con penetración eólica

Ernesto Jair Eguis-Eslava [1]; Kelly Marcela Padilla-García [2];
Luis Alberto López-Díaz [3]; José Daniel Soto-Ortiz [4]; Rafael Castillo-Sierra [5];
Mauricio Pardo-González [6]; Cesar Augusto Orozco-Henao [7];
Elvin Arnaldo Jiménez-Matos [8]; Ingrid Oliveros-Pantoja [9]

[1] BSc. In Electrician Engineering, Universidad del Norte, Colombia. Current position: Proinges SAS, Colombia. E-mail: eeguis@uninorte.edu.co ORCID: https://orcid.org/0000-0002-4975-3439

[2] BSc. In Electrician Engineering, Universidad del Norte, Colombia. Current position: Zona Franca Celsia, Colombia. E-mail: kmpadilla@uninorte.edu.co ORCID: https://orcid.org/0000-0002-8706-2778

[3] BSc. In Electrician Engineering, Universidad del Norte. Universidad del Norte, Colombia. E-mail: llopeza@uninorte.edu.co ORCID: https://orcid.org/0000-0002-6436-0916

[4] BSc. In Electrician Engineering, Universidad Técnica de Georgia, Georgia. MSc. Universidad Técnica de Georgia, Georgia. Current position: Universidad del Norte, Colombia. E-mail: jsoto@uninorte.edu.co ORCID: https://orcid.org/0000-0002-1143-7844

[5] BSc. In Electrician Engineering, Universidad del Norte, Colombia. MSc. Universidad del Norte, Colombia. Current position: Universidad del Norte, Colombia. E-mail: rcastillo@uninorte.edu.co ORCID: https://orcid.org/0000-0002-2648-4096

[6] BSc. In Electronic Engineering, Universidad del Norte, Colombia. PhD. Instituto de Tecnología de Georgia, Georgia. Current position: Universidad del Norte, Colombia. E-mail: mpardo@uninorte.edu.co ORCID: https://orcid.org/0000-0002-7608-3290

[7] BSc. In Electrician Engineering, Universidad Tecnológica de Pereira, Colombia. PhD. Universidad Federal de Rio Grande del Sur, Brasil. Current position: Universidad del Norte, Colombia. E-mail: chenaoa@uninorte.edu.co ORCID: https://orcid.org/0000-0002-8184-6205

[8] BSc. In Electrician Engineering, Instituto Tecnológico de Santo Domingo, República Dominicana. MSc. Politécnica de Madrid, España. Current position: Instituto Tecnológico de Santo Domingo, República Dominicana. E-mail: elvin.jimenez@intec.edu.co ORCID: https://orcid.org/0000-0002-0031-6772

[9] BSc. In Electrician Engineering, Universidad del Norte, Colombia. PhD. Politécnica de Madrid, España. Current position: Universidad del Norte, Colombia. E-mail: inoliver@uninorte.edu.co. ORCID: https://orcid.org/0000-0002-1488-2089

Abstract: This article presents the results of the analysis of the studies of the operation of a modified IEEE-13 distribution feeder, which was built to scale in the laboratory at Universidad del Norte. In this article, we show the cases of the operating regimes of the modified IEEE-13, before the different levels of wind energy penetration. The modified IEEE-13 distribution feeder was built taking into account that each of the scaled modules and their generator-load will work under the conditions of the Universidad del Norte laboratory. An experimental methodology was used to compare the results obtained in the actual scaled model with the results of the simulations in specialized programs. The conclusions of the article show the wind energy that can be injected into an electrical system with conventional power generation so that it can maintain its operation complying with the current regulatory framework.

Keywords: Distributed Generation, Electrical Losses, Energy Efficiency, IEEE-13, Renewable Energies, Wind energy.

Resumen: En este artículo se presentan los resultados del análisis de los estudios de la operación de un alimentador de distribución IEEE-13 modificado, que fue construido a escala en el laboratorio en la Universidad del Norte. En este artículo, se muestran los casos de los regímenes de operación del IEEE-13 modificado, ante los diferentes niveles de penetración de energía eólica. Este alimentador de distribución IEEE-13 modificado se construyó teniendo en cuenta que cada uno de los módulos escalados y su generador-carga funcionarán en las condiciones particulares del laboratorio de la Universidad del Norte. Se utilizó una metodología experimental que, para la comparación de los resultados obtenidos en el modelo real escalado, con los resultados de las simulaciones en programas especializados. Se pudo definir la

cantidad de energía eólica que se puede inyectar a un sistema eléctrico con generación de energía convencional, de modo que pueda mantener su funcionamiento, no sólo respetando las condiciones técnicas, sino también bajo el estricto cumplimiento de un marco regulatorio.

Palabras clave: Generación Distribuida, Pérdidas Eléctricas, Eficiencia Energética, IEEE-13, Energías Renovables, Energía Eólica.

1. Introduction

The installed capacity of electricity generation in the Non-Interconnected Zones (ZNI for its acronym in Spanish) in Colombia is 99.9% by diesel generation. The access to electricity in the ZNI is deficient and has an expensive service; where its real cost corresponds to twice the average cost of the kWh of the National Interconnected System, with the aggravating circumstance that it only receives service half of the hours of the day [1]. For this reason, it is planned to achieve a contribution of 30% of the installed capacity of electricity generation with non-conventional energies in the ZNI by 2020. This is supported by the law 1715 of 2014, which promotes the use of non-conventional sources of energy, mainly in ZNI, with the purpose of strengthening the national energy supply, under a sustainable economic framework [2].

The high levels of penetration of renewable energies in conventional distribution systems present a new challenge in the normal operation of the system [3]. Several authors have centered their work on an integration of distribution systems with emerging renewable technologies, including distributed wind generation [4]–[6]. The distributed wind generation resource modifies the normal operation of the system due to its inherent intermittency and its limited capacity to deliver reactive power to the network [7]. In [8] Méndez et al., they evaluate

the performance of the losses of the distribution system due to the high penetration of distributed generation in the network. The authors present an approach to calculate annualized losses in the system due to the different levels of penetration and concentration of wind energy in the system.

In [4] Moustafa et al., they propose a methodology for the optimal integration of distributed generation with wind resource and energy storage systems. In the discussion, it is shown that the intermittency of wind power generation systems affects the operating costs of the distribution system for the companies providing the service. This increase in costs occurs when the penetration of wind energy in the distribution system increases. Therefore, the proposal is aimed at optimally locating energy storage systems that mitigate the intermittency of distributed wind generation subject to technical constraints.

In [9] Ahmadi and Ghasemi propose a method to determine the maximum penetration level of wind farms based on synchronous machines and doubly fed induction machines. Considering the random nature of the wind speed, the article performs a transient stability analysis to determine the maximum penetration level of the wind farms. The obtained results show that the high penetration of wind generators produces a reduction of the general inertia of the system for which the authors propose a methodology based on a unit commitment with restrictions due to the wind farms.

In [10] Liew and Strbac study the embedded wind generation connection in a rural type distribution system. Rural distribution systems have the particular of covering large distances and having scattered loads. This particularity presents a challenge to maximize the benefits of wind generation and transform conventional distribution systems into active distribution

systems. The authors present three insertion strategies that are evaluated throughout the research work: Wind generation during periods of low demand, wind generation with compensation of reactive power and wind generation with change control of tap transformers. Other lines of research are focused on system variables such as power quality, operating costs and the risks associated with the integration of distributed wind generation. In [11] Mahela et al., They study the power quality in distribution networks with high wind penetration. In [12] Zubo et al., Present a distribution market proposal for the integration of networks with high penetration of wind and solar energy. In [13] Chang et al., they evaluate the risks associated with the high penetration of wind farms in the transmission systems and generators already installed in the network.

The strategic area of the energy of the Universidad del Norte has developed a microgrid, which was planned to recreate real operating scenarios similar to the networks of the ZNI [14]. The microgrid has generation modules that emulate non-conventional energy sources. The contributions of the wind profiles are modeled and simulated, where the different operating conditions were studied. The microgrid and its generation modules allow evaluating variables such as energy efficiency, the increase in the use of non-conventional renewable energies, the reduction of greenhouse gas emissions, the increase in security of supply and the minimization of electrical losses.

The designed microgrid is scaled up to the voltage level of 220 V. The local distribution network and the emulators compose the micro-grid based on the IEEE-13 standard. In addition, a model was developed with specialized software, in order to evaluate the network before different

Preparación de Artículos revista VISIÓN ELECTRÓNICA: algo más que un estado sólido
Fecha de envío: 10 de septiembre de 2018
Fecha de recepción: 27 de septiembre de 2018
Fecha de aceptación: 25 de octubre de 2018

operating scenarios, these being: steady-state study connected and isolated from the Local

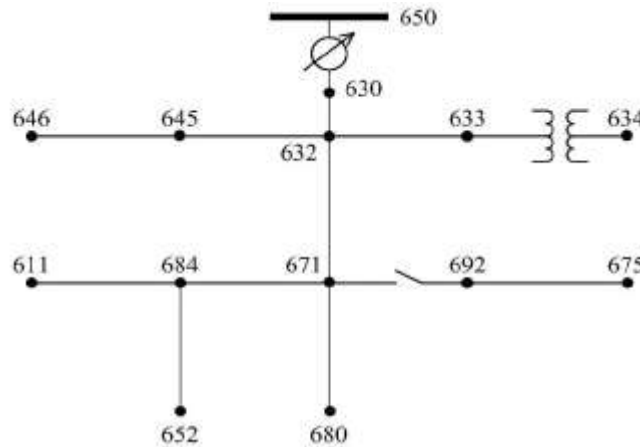Distribution Network (LDN) and the study in the isolated dynamic state of the network.

Figure 1. Modified IEEE 13 one-line diagram. Source: own.

2. Basic design of the microgrid

2.1. Topology selection

The distribution network model was selected according to the IEEE-13 test feeder and was

adapted for laboratory work, as shown in Figure 1.

2.2. Wind speed study

The measurements made of the wind speeds allowed to elaborate a statistical profile. With the

historical data, the measures of central tendency and dispersion were calculated for the data

set in the months of record. In this manner, it was possible to know the distribution of the

frequency of the winds, as shown in Figure 2. We identified 18 wind speeds. The wind speed
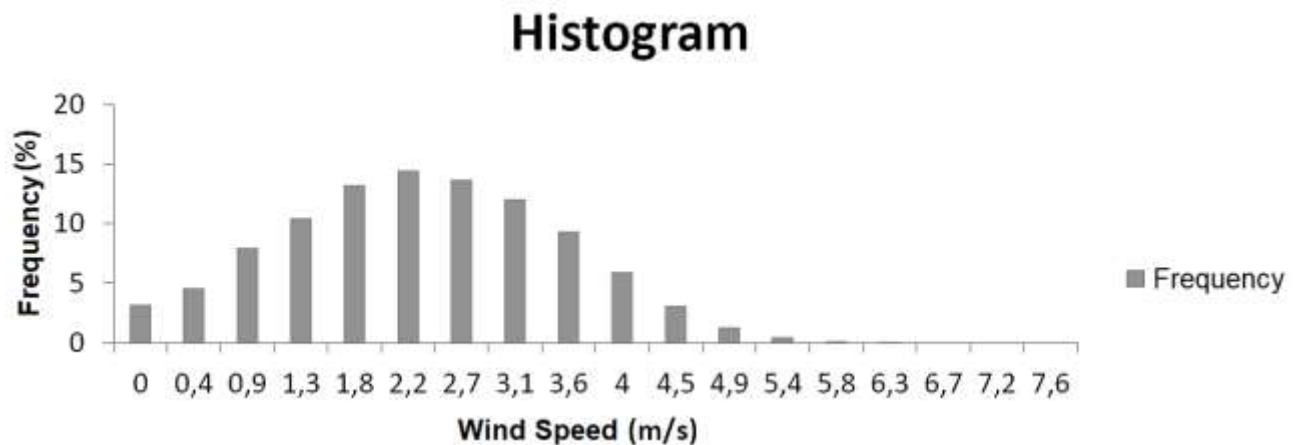
with the highest frequency was 2.2 m/s.

Figure 2. Wind speed histogram. Source: own.

2.3. Characteristics of the wind turbine and diesel generator

The ENAIR wind turbine was selected for its efficiency, design and its capacity to generate electricity at considerably low wind speeds [15]. The wind turbine has a starting speed of 1.8 m/s and an efficient generation range of 2 to 60 m/s, with a nominal power of 1900 W. The machine operates according to IEC 61400 class IA [16]. In addition, it has a controller for charging batteries and its connection to the local network.

The wind turbines and the diesel plant were characterized according to the modified model of the IEEE-13 standard. In this sense, the plant was modeled with the characteristics of the synchronous generators of the LEM (Laboratory of Electrical Machines) of the Universidad del Norte. On the other hand, for wind turbines, the factor and power curve of the machine were specified, as well as its nominal voltage and power. Next, in Figure 3, the simulated system is presented in specialized software, in connection with the wind turbines and the diesel plant.
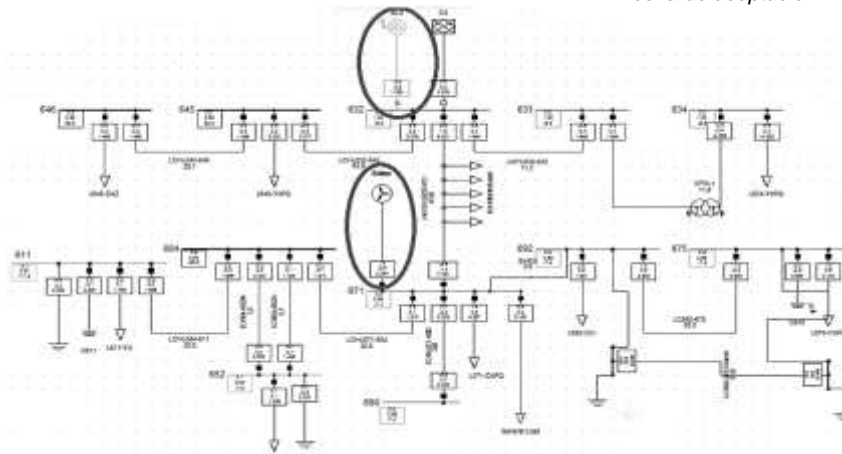
Preparación de Artículos revista VISIÓN ELECTRÓNICA: algo más que un estado sólido
Fecha de envío: 10 de septiembre de 2018
Fecha de recepción: 27 de septiembre de 2018
Fecha de aceptación: 25 de octubre de 2018

Figure 3. Software model of IEEE-13 Test feeder. Source: own.

3. Wind energy generation

The wind potential was determined by the environmental characteristics of the site and the technical characteristics of the selected wind turbine, using the Weibull distribution as shown in Figure 4. The wind turbine has a sweep radius of 1.9 m, which allowed it to reach a power of 1155.45 W in the seven months of data collection (Table 1). The analysis of the wind speed, estimating the energy that the wind turbine could generate per month is shown in Table 2.
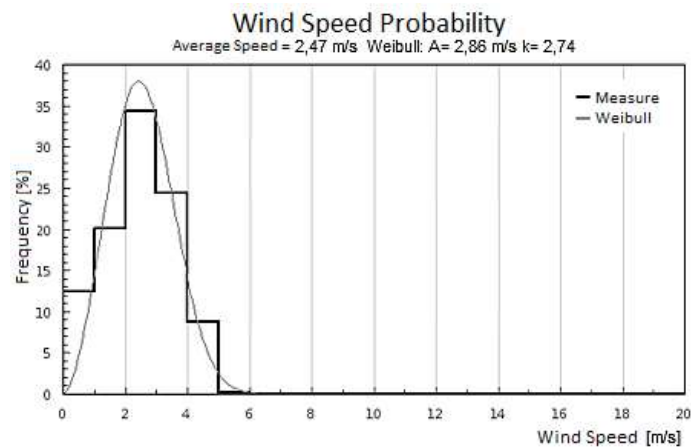

Figure 4. Wind speed probability distribution. Source: own.

Month	Wind Power (W)
October	28,227
November	23,779
December	148,892
January	234,286
February	247,380
March	317,574
April	155,318
Total	1155,45

Table 1. Wind turbine power ENAIR E30 Pro. Source: own.

Month	Average energy 24h per month (Wh)	Energy peak (Wh)	Hour
October	524,56	48,14	1:00 - 1:55 pm
November	509,62	53,12	1:00 - 1:55 pm
December	2693,35	169,32	4:00 - 4:55 pm
January	4125,93	243,19	12:00 - 12:55 pm
February	4097,71	261,45	3:00 - 3:55 pm
March	5039,76	296,31	2:00 - 2:55 pm
April	2623,63	224,93	3:00 - 3:55 pm

Table 2. Wind energy per month. Source: own.

4. Design of experiments

For the design of the experiment, 4 case studies were established (Table 3) based on 3 criteria, taking into account the location in the microgrid of non-conventional generation sources. In the first criterion, the monophasic and biphasic nodes are not considered as possible connection points. Also, as a second criterion, node 632 is not taken into account for the inclusion of renewable sources, since it is the point of connection of the microgrid to the network and node 632 is the connection point of the diesel plant for the isolated case. Finally, the third criterion

considers the distance between the renewable source and the demand points. The wind

turbines are located in those nodes that present the highest demand, in order to minimize losses

and voltage drops.

Case 1 -	Distributed generation concentrated in node 680. Node without generation or initial demand.
Case 2 -	Generation distributed in nodes 633, 671 and 675. Three-phase nodes close to demand.
Case 3 -	Distributed centralized generation in node 671. Central node in the network. In addition, the largest centralized demand in the network (33.3% of total active power demand).
Case 4 -	Distributed generation centralized in node 675. The node with the second highest demand (24.3% of the total active demand of the network).

Table 3. Case study. Source: own.

In the framework of the previous observations, the tests of the wind models in the transient

simulations led to the conclusion that the existing models would provide an acceptable

response to the transient voltage tests, however, they were not suitable for the stability test of

the small signal [17].

5. Analysis and results

5.1. Steady-state study: connected and isolated to the distribution network

In this section, we present the simulations of the steady-state: system connected and isolated

to the LDN, and two methods were used for data analysis. The first of the methods consists of

the analysis of the response variables of the system before each case study. The second

method selected the case study with the best response to the inclusion of wind generation in

the network. The results presented below were obtained by the first method.

5.1.1. Voltage analysis

The voltages of phase A, which are shown in Figure 5, are within the range established by the Comisión de Regulación de Energía y Gas CREG 024 de 2005 [18] under the injection of the renewable source to the network. The voltages of phase B presented a negative response to the increase in the power injection of the wind turbines. Phase B presented the same tendency as the others (increase in voltage in the nodes near the power injection point). However, the increase in voltage at B resulted in relatively significant overvoltage at nodes 671, 675, 692 and 680.
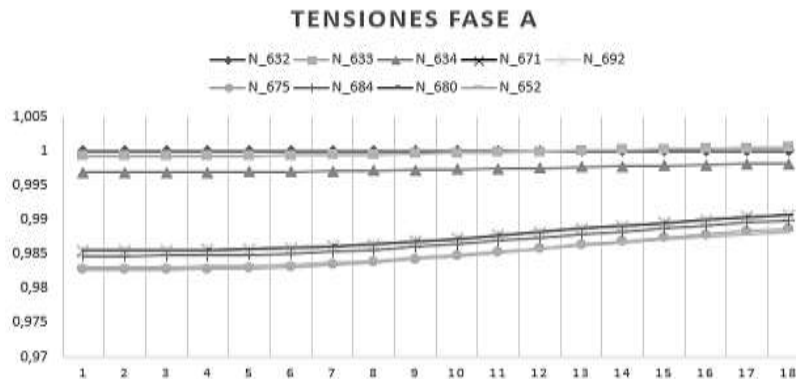

Figure 5. Voltage phase A – Case 2. Source: own.

The voltages of phase C presented a consistent response between the different case studies; the behavior trend was the increase in the tension of the nodes that presented the worst regulation values (nodes 671, 692, 675, 680, 684, 652 and 611). On the other hand, the nodes that presented the best regulation values (645, 646, 633 and 634) maintained almost constant voltage values against the changes of active wind power injected into the network.

5.1.2. Loadability lines analysis

Case 1: The increase in wind generation ended in a decrease in current on line 632-671. At the same time, there was an increase in current on line 671-680, because all the wind generation was concentrated in node 680. Even so, no overloads are generated in this case study.

Case 2: The distribution of wind generation in the network had a more significant response in the system. The loadability of lines 632-671, 632-633 and 692-675 was reduced to the point where the generation of wind turbines exceeded local demand and began to provide power to the rest of the system. However, it should be clarified that in the present case study there were no violations of operating conditions due to overloads in the lines.

Case 3: This case did not present a greater contribution than decreasing the flow transported by line 632-671. No overloads on the lines were generated.

Case 4: Line 632-671 showed a decrease in the current while the current on line 692-675 was decreased; because the demand located in node 675 began to be supplied by wind turbines. With a high penetration, the current of line 692-671 increased its loadability, but with an inverse flow to that presented before. In this case, there was an overload of 120% of the nominal value of the line.

5.1.3. Power loss analysis

The response of the system to the inclusion of renewable energies was given as a decrease in the total losses of the system (within the wind ranges studied). Figure 6 shows that case studies 3 and 4 show the lowest values in their loss curves.
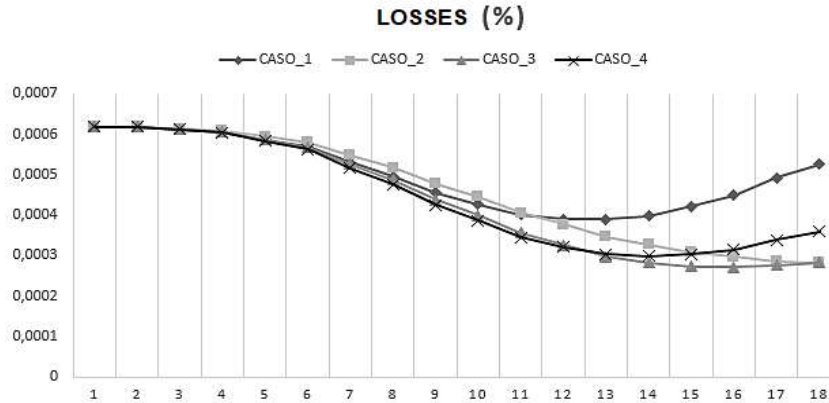
Figure 6. Power losses of the system before the inclusion of renewable. Source: own.

During the development of the study method, a statistical analysis of each of the response variables of the system was carried out. First, we proceeded to the study of voltages; for this, Root Mean Square Error (RMSE) was calculated for each case. In this sense, the error or difference between the voltages of every node along the iterative process of the DPL (DIgSILENT Programming Language) with reference to the ideal voltage (1 p.u) was calculated. Next, (1) was used to calculate the RMSE of every node.

$$RMSE = \sqrt{\frac{1}{n}\sum_{j=1}^{n}|V_{ref} - V_j|^2}$$
(1)

Where:

n: Number of iterations (18 iterations).

Vj: voltage node at iteration j.

$Vref$: Reference value of the voltage (1 p.u.).

Thus, in 67% of the nodes of phase A, case study 4 presented the smallest deviations with reference to the tension of 1 p.u .; while, in the second case study, the lowest RMSE values

were presented in the remaining nodes, as shown in Table 4. The voltages of phase b have the

same response. The second case studied was the one that presented the lowest RMSE values

(67% of the nodes) shown in Table 5.

RMSE Voltage Phase A				
NODE	**CASE 1**	**CASE 2**	**CASE 3**	**CASE 4**
N_632	0	0	0	0
N_633	0,0732	0,0498	0,0732	0,0731
N_634	0,3115	0,2648	0,3115	0,3114
N_671	1,1895	1,2643	1,1866	1,1853
N_692	1,1895	1,2643	1,1866	1,1853
N_675	1,4630	1,5150	1,4599	1,3890
N_684	1,2672	1,3429	1,2642	1,2629
N_680	1,0952	1,2642	1,1866	1,1853
N_652	1,4261	1,5035	1,4230	1,4216

Table 4. RMSE Voltage Phase A. Source: own.

RMSE Voltage Phase B				
NODE	**CASE 1**	**CASE 2**	**CASE 3**	**CASE 4**
N_632	0	0	0	0
N_645	0,3375	0,3375	0,3375	0,3375
N_646	0,4112	0,4112	0,4112	0,4112
N_633	0,1056	0,0706	0,1057	0,1058
N_634	0,2939	0,2463	0,2940	0,2941
N_671	0,2785	0,2463	0,2837	0,2813
N_692	0,2785	0,2463	0,2837	0,2813
N_675	0,4264	0,4244	0,4312	0,5179
N_680	0,3342	0,2463	0,2837	0,2813

Table 5. RMSE Voltage Phase A. Source: own.

Table 6 shows the values of phase c voltage, in which 50% of the nodes had lower values of

RMSE in the fourth case study. In contrast, 20% of the remaining nodes had a better response

in the second case study and only 10% obtained the best stress values in the first case study.

NODE	CASE 1	CASE 2	CASE 3	CASE 4
RMSE Voltage Phase C				
N_632	0	0	0	0
N_645	0,0015	0,0015	0,0015	0,0015
N_646	0,0024	0,0024	0,0024	0,0024
N_633	0,0017	0,0012	0,0017	0,0017
N_634	0,0039	0,0033	0,0039	0,0039
N_671	0,0172	0,0179	0,0172	0,0172
N_692	0,0172	0,0179	0,0172	0,0172
N_675	0,0184	0,0190	0,0184	0,0179
N_684	0,0182	0,0189	0,0181	0,0181
N_611	0,0190	0,0197	0,0189	0,0189
N_680	0,0162	0,0179	0,0172	0,0172

Table 6. RMSE Voltage Phase C. Source: own.

Summary, voltages nodes of the microgrid presented the best response to the inclusion of wind sources in Case 4, where the lowest RMSE values were obtained in 62% of voltages analyzed. Subsequently, the analysis of the loadability of the microgrid lines was carried out. Table 7 shows the overload that occurred in case 4, due to the overload generated in line 675-692.

	LOADABILITY (%)	AVERAGE POWER LOSSES (%)
CASE 1	69,189	0,000499
CASE 2	70,447	0,000459
CASE 3	70,447	0,000435
CASE 4	120,467	0,000444

Table 7. Maximum loadability and average power losses. Source: own.

Additionally, Table 7 shows the average total losses expressed in a percentage that was obtained. Specifically, the third case study does not outrage the loadability restrictions of the conductors of the lines, likewise, it has the second best voltage response and presents the

lowest losses. Therefore, the dynamic study will analyze the centralized wind generation in node 671.

The results presented so far correspond to the scenario where the microgrid operates connected to the local distribution network. Likewise, steady-state studies were carried out for an isolated case. The difference between the response of the system operating in isolation and connected is not significant.

5.2. Dynamic study isolated to the distribution network

RMS simulations were carried out in which the frequency and voltage response of the system was analyzed under the fluctuation of the wind and demand. First, the dynamic study of the system was carried out under fluctuations in wind speed. In Figure 7, the histogram of the wind speed changes between two continuous measurements is shown. On the other hand, in Figure 7 it is possible to observe that the greatest variation between wind speeds recorded between two continuous measurements is 3.6 m/s.
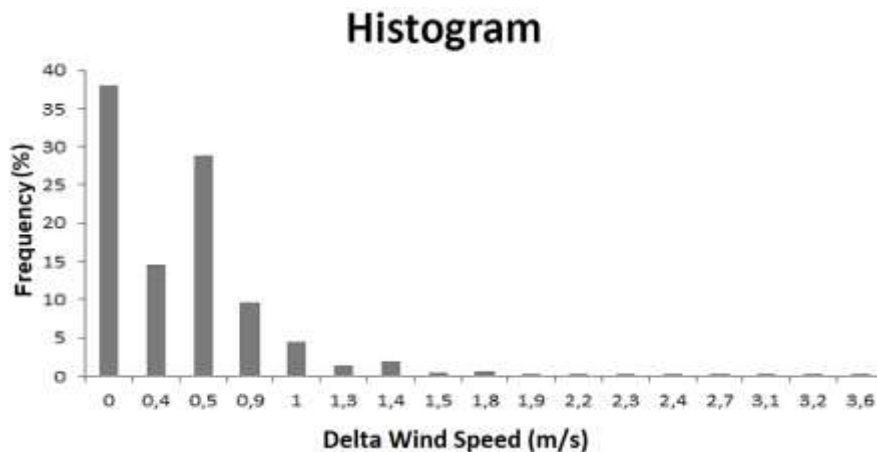

Figure 7. Histogram of variations in recorded wind speeds. Source: own.

Initially, the response of the system to the variation of power generated by three wind turbines was simulated. Therefore, the power swap to which the network was subjected was 2520 W in 5 minutes (8.4 W/s). Based on the above considerations, the results were as follows.
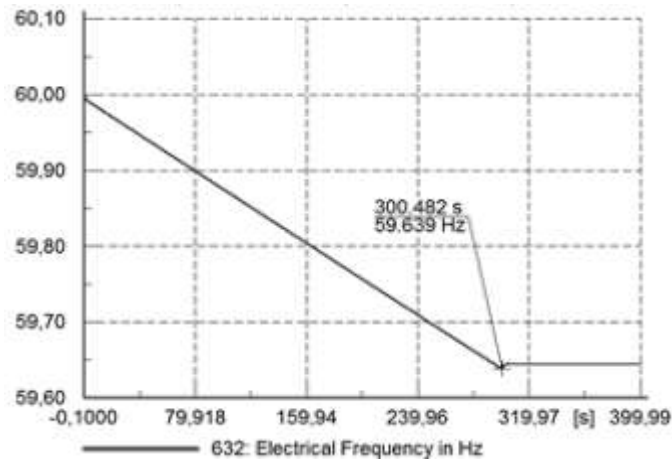

Figure 8. Frequency response in the critical change with 2 wind turbines. Source: own.

When the network is governed to the change of power generated by the wind turbines, a progressive imbalance between generation and demand originates. For this case, at the end of the loading event, the frequency had a value of 59,468 Hz.
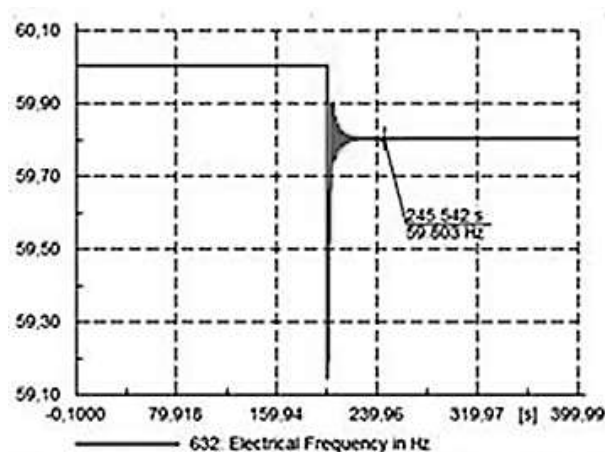

Figure 9. Frequency response to a power change of 22%. Source: own.

On the other hand, the inertia of the system added to that of the diesel generator did not manage to maintain the system under acceptable operating conditions faced to the variation of the power of three wind turbines. For this reason, the same analysis was carried out with two wind turbines. Figure 8 shows the frequency results of this event.

In fact, given that the conditions for frequency regulation were not reached, the system analysis was carried out with a single wind turbine, where the response shown in Figure 9 was obtained.

Total Demand (W)	Power demand change (%)	Power demand change(W)	Frequency (Hz)
4243	10%	424,3	59,91
	20%	848,6	59,82
	22%	933,46	59,8

Table 8. Frequency response to sudden changes in demand. Source: own.

Consequently, the largest instantaneous change such that the system can stay within the ranges accepted by the distribution system design standard [19] is 934 W. In fact, power changes that exceed 22% of the demand of the system affect changes in frequency. The aforementioned data are shown in Table 8.

6. Conclusions and recommendations

First, historical wind data analysis was carried out at Universidad del Norte, whose results showed low wind speeds compared to those required to support the proposed microgrid. The power and energy generated by the wind turbines were minimal for the requirements of the microgrid. Wind potentials are less than 10% of the total demand of the system. The greatest potential recorded was in the month of March with a total of 317.5 W and the power demanded

by the system is 4228 W. The highest generation peak with 296.31 Wh occurred during the month of March, too. In relation to the losses that occur when incorporating renewable energies to the system, it can be concluded that these are minimized by having a wind contribution. In the system, the presented variations were within a range of ± 0.005 p.u.

Analyzing the different case studies, the best connection point for the wind generators is node 671, because it presented the lowest percentages of losses, there were no overloads in the lines and, in addition, the voltages nodes remained within the range established by legislation.

In the same way, by applying direct injection to the network by wind turbines and studying the frequency response of the system, it was concluded that the number of wind turbines that can be implemented is limited to one; otherwise, the conditions of stability would be violated due to the fluctuations of power injected by the wind turbines

Finally, the sudden change in demand that may occur, such that the frequency does not exceed the regulatory ranges is 934 W, which represents a change in demand equal to 22%.

7. Acknowledgments

References

[1] J. Flórez, D. Tobón and G. Castillo, "¿Ha sido efectiva la promoción de soluciones energéticas en las zonas no interconectadas (ZNI) en Colombia?: un análisis de la estructura institucional", *Cuadernos de administración*, vol. 22, no. 38, 2009, pp. 219–245.

[2] Congreso de Colombia, "Ley 1715. Mayo 2014", 2014. [Online]. Available at: http://www.secretariasenado.gov.co/senado/basedoc/ley_1715_2014.html

[3] G. Pepermans, J. Driesen, D. Haeseldonckx, R. Belmans and W. D'haeseleer, "Distributed generation: Definition, benefits and issues", *Energy Policy*, vol. 33, no. 6, 2005, pp. 787–798. https://doi.org/10.1016/j.enpol.2003.10.004

[4] Y. M. Atwa and E. F. El-Saadany, "Optimal allocation of ESS in distribution systems with a high penetration of wind energy", *IEEE Trans. Power Syst.*, vol. 25, no. 4, 2010, pp. 1815–1822. https://doi.org/10.1109/TPWRS.2010.2045663

[5] M. R. Baghayipour, A. Hajizadeh, A. Shahirinia and Z. Chen, "Dynamic placement analysis of wind power generation units in distribution power systems", *Energies*, vol. 11, no. 9, 2018, pp. 1–16. https://doi.org/10.3390/en11092326

[6] K. Maki, "Effect of wind power based distributed generation on protection of distribution network", Eighth IEEE International Conference on Developments in Power System Protection, 2005, pp. 327–330. https://doi.org/10.1049/cp:20040129

[7] T. R. Ayodele, A. Jimoh, J. L. Munda and A. J. Tehile, "Challenges of Grid Integration of Wind Power on Power System Grid Integrity: A Review", *Int. J. Renew. Energy Res.*, vol. 2, no. 4, 2012, pp. 618–626.

[8] V. Mendez, J. Rivier and T. Gomez, "Assessment of Energy Distribution Losses for Increasing Penetration of Distributed Generation", *IEEE Trans. Power Syst.*, vol. 21, no. 2, 2006, pp. 533–540. https://doi.org/10.1109/TPWRS.2006.873115

[9] H. Ahmadi and H. Ghasemi, "Maximum penetration level of wind generation considering power system security limits", *IET Gener. Transm. Distrib.*, vol. 6, no. 11, 2012, pp. 1164–1170.

[10] S. N. Liew and G. Strbac, "Maximising penetration of wind generation in existing distribution networks", *IEEE Proc. - Gener. Transm. Distrib.*, vol. 149, no. 3, 2002, pp. 256-262.

[11] O. P. Mahela, P. Prajapati and S. Ali, "Investigation of Power Quality Events in Distribution Network with Wind Energy Penetration", IEEE Int. Students' Conf. Electr. Electron. Comput. Sci. SCEECS, 2018, pp. 1–5. https://doi.org/10.1109/SCEECS.2018.8546945

[12] R. H. A. Zubo, G. Mokryani and R. Abd-Alhameed, "Optimal operation of distribution networks with high penetration of wind and solar power within a joint active and reactive distribution market environment", *Appl. Energy*, vol. 220, 2018, pp. 713–722. https://doi.org/10.1016/j.apenergy.2018.02.016

[13]   Y. Chang *et al.*, "Risk Assessment of Generation and Transmission Systems Considering Wind Power Penetration", Int. Conf. Power Syst. Technol. POWERCON, 2018, pp. 1169–1176. https://doi.org/10.1109/POWERCON.2018.8601737

[14]   P. De la Hoz, A. Silva, R. Castillo-sierra, I. Oliveros, M. Pardo and E. Jimenez, "UniGRID: Photovoltaic Study Case for the Universidad del Norte Renewable Energies", 15th International Conference on Electrical Engineering, Computing Science and Automatic Control (CCE), 2018, pp. 1–6. https://doi.org/10.1109/ICEEE.2018.8533985

[15]   ENAIR, "Aerogenerador ENAIR E30 PRO Ficha Técnica" [Online]. Available at: https://www.enair.es/es/Aerogeneradores/E30PRO

[16]   IEC, "IEC International Standard 61400-1", 2008, pp. 1–9. [Online]. Available at: https://webstore.iec.ch/preview/info_iec61400-1%7Bed3.0%7Den.pdf

[17]   J. Conto, "Grid challenges on high penetration levels of wind power", IEEE Power Energy Soc. Gen. Meet., 2012, pp. 1–3. https://doi.org/10.1109/PESGM.2012.6344717

[18]   Comisión de Regulación de Energía y Gas - CREG, "Resolución No. 024 de 2005", 2005. [Online]. Available at: http://www.creg.gov.co/html/Ncompila/htdocs/Documentos/Energia/docs/resolucion_creg_0024_2005.htm.

[19]   Empresa Electrificadora de Santander ESSA, "Norma Técnica ESSA, "Normas para cálculo y diseño de sistemas de distribución", 2004. [Online]. Available at: https://www.essa.com.co/site/Portals/14/Docs/Norma%20tecnica/Norma%20T%C3%A9cnica%20ESSA.pdf